

High Galactic latitude *Fermi* sources of γ -rays with energies above 100 GeV.

A. Neronov¹, D.Semikoz^{2,3} and Ie.Vovk¹

¹ ISDC Data Centre for Astrophysics, Ch. d'Ecogia 16, 1290, Versoix, Switzerland
e-mail: Andrii.Neronov@unige.ch

² APC, 10 rue Alice Domon et Leonie Duquet, F-75205 Paris Cedex 13, France

³ Institute for Nuclear Research RAS, 60th October Anniversary prosp. 7a, Moscow, 117312, Russia
e-mail: Dmitri Semikoz <dmitri.semikoz@apc.univ-paris7.fr>

Preprint online version: April 22, 2010

ABSTRACT

Aims. We present a catalog of sources of very high energy ($E > 100$ GeV) γ -rays detected by *Fermi* telescope at Galactic latitudes $|b| \geq 10^\circ$.

Methods. We cross correlate the directions of individual photons with energies above 100 GeV detected by *Fermi* with the catalog of sources detected at lower energies. We find significant correlation between the arrival directions of the highest energy photons and positions of *Fermi* sources, with the possibility of chance coincidences at the level of 10^{-38} . We present a list of *Fermi* sources contributing to the correlation signal. A similar analysis is done for cross-correlation of the catalog of BL Lac objects with the highest energy photons detected by *Fermi*.

Results. We produce a catalog of high Galactic latitude *Fermi* sources visible above 100 GeV. The catalog is split onto two parts. First part contains a list of 46 higher significance sources among which there can be 2 or 3 possible false detections. Second part of the catalog contains a list of 21 lower significance sources, among which 5 or 6 are possibly false detections. Finally we identify 7 additional sources from the cross-correlation analysis with the BL Lac catalog. The reported sources of $E > 100$ GeV γ -rays span a broad range of redshifts, up to $z \sim 1$. Most of the sources are BL Lac type objects. Only 16 out of 74 objects in our list were previously reported as VHE γ -ray sources.

Key words. Catalogs – Gamma rays: galaxies – Galaxies: active – BL Lacertae objects: general

1. Introduction

Ground-based Cherenkov γ -ray telescopes HESS, MAGIC and VERITAS have discovered a population of sources of Very High Energy (VHE) ($E \geq 100$ GeV) γ -rays. Except for the sources discovered in the Galactic Plane survey by HESS (Aharonian et al., 2005, 2006), most of the sources were discovered in dedicated pointed observations. Surveys of large regions of the VHE γ -ray sky with the existing Cherenkov telescopes are difficult because of the too narrow size of the field of view. Wide field of view ground-based γ -ray detectors MILAGRO (Atkins et al., 2004) and Tibet (Amenomori et al., 2005) arrays have produced a systematic survey of the VHE γ -ray sky. The energy threshold of the air shower arrays like MILAGRO and TIBET is rather high (in the multi-TeV band) so that only sources with spectra extending well above 1 TeV could be detected.

All-sky monitoring of γ -ray sources at the energies $E \sim 100$ GeV became possible with the start of operation of *Fermi* telescope. Space-based *Fermi* telescope has a much smaller effective collection area, compared to the ground based γ -ray telescopes (~ 1 m², compared to $\sim 10^5$ m² for the ground-based γ -ray telescopes). At the same time, at the energies above 100 GeV *Fermi* signal is almost background-free (contrary to the ground based telescopes in which the signal has to be identified on top of strong background created by cosmic rays and optical/UV night sky background). Neronov et al. (2010) have searched for the point sources of $E \geq 100$ GeV γ -rays using *Fermi* data and found

8 significant excesses with at least 3 photons within 0.1° circle corresponding to the 68% containment radius of point spread function (PSF) of the Large Area Telescope (LAT) on board of *Fermi*. Seven excesses were associated with known VHE γ -ray sources, while the remaining one was identified with head-tail radio galaxy IC 310. Detection of IC 310 in the VHE band was later confirmed by MAGIC telescope (Mariotti, 2010). Due to the moderate collection area of *Fermi*, only the brightest VHE γ -ray sources were detected individually in the *Fermi* VHE γ -ray sky survey. All other known VHE γ -ray sources at Galactic latitudes $|b| \geq 10^\circ$ gave ≤ 2 photons within the LAT PSF circle and could not be found from the analysis of the data above 100 GeV alone.

A complementary method to identify the sources of $E \geq 100$ GeV photons detected by *Fermi* is to use a prior knowledge of source positions on the sky and to verify which of the already known sources could have produced the highest energy γ -rays detected by the LAT telescope. In other words, sources of $E \geq 100$ GeV γ -rays could be identified also via cross-correlation of arrival directions of the $E \geq 100$ GeV γ -rays with the source positions on the sky. Such an approach to the identification of the sources was previously applied to the analysis of EGRET data above 10 GeV by Dingus & Bretsch (2001) and Gorbunov et al. (2005).

In what follows we perform the cross-correlation analysis of the arrival directions of γ -rays with energies above 100 GeV detected by *Fermi* at Galactic latitudes $|b| \geq 10^\circ$ with the 1-st year *Fermi* source catalog (Abdo et al., 2010a). Our analysis results

in a catalog of 46 high Galactic latitude sources of $E \geq 100$ GeV γ -rays. Although each individual source in the catalog is detected with significance around 3σ in this energy band, overall significance of detection of the entire source set is very high. Simple analysis shows that most of the sources contributing to the correlation signal are real VHE γ -ray sources, only 2 or 3 of them are expected to be false detections. Taking into account the fact that most of the sources in the list are BL Lac type objects, we extend our cross-correlation analysis to the catalog of BL Lacs (Veron-Cetty & Veron, 2010) and find 7 more sources which correlate with the arrival directions of $E \geq 100$ GeV γ -rays and are not listed in the 1-st year *Fermi* catalog. Finally, we list for completeness sources from the 1-st year *Fermi* catalog for which the $E \geq 100$ GeV γ -rays are found within the 95%, rather than 68% containment circle of LAT PSF. There are 21 such sources, 5 or 6 of them are expected to be false detections due to the chance coincidence of the arrival direction of the VHE γ -ray with the source position.

The plan of the paper is like follows. In Section 2 we discuss data selection and data analysis methods. In Section 3 we present the results of the correlation analysis of the arrival directions of $E \geq 100$ GeV γ -rays with the sources of the 1-st year *Fermi* catalog. In Section 4 we give the list of sources contributing to the correlation signal. In Section 5 we perform the correlation analysis with the BL Lac catalog of Veron-Cetty & Veron (2010) and give the list of additional BL Lacs correlating with the highest energy *Fermi* photons, but not present in the 1-st year *Fermi* catalog. In Section 6 we comment upon individual sources. Finally, in Section 7 we discuss the results.

2. Data selection and data analysis

For our analysis we have used the LAT data which were collected in the period between August 4, 2008 and April 12, 2010. The data were filtered using *gtselect* tool, so that only γ -ray events (*evcls*=3) with energies above 100 GeV were retained for the analysis. The resulting list of photons has 4427 events. A fraction of the $E \geq 100$ GeV photons comes from the directions close to the Galactic Plane. Galactic Plane is a source of significant diffuse γ -ray emission even at the energies higher than 100 GeV. Presence of strong diffuse emission complicates the analysis of the point source contribution. Taking this into account we consider only photons coming from Galactic latitudes $|b| \geq 10^\circ$. The cut on the Galactic latitude leaves 2774 photons for the analysis.

The set of photons considered in the analysis includes the list of photons studied by Neronov et al. (2010). In our analysis we exclude the high-confidence sources of VHE γ -rays identified by Neronov et al. (2010). We also exclude 65 γ -rays associated to these 8 sources from the *Fermi* $E \geq 100$ GeV photon list. Otherwise, these sources would dominate the correlation signal. Nevertheless, we include the high-confidence sources in the final source list given in the Table 1, to obtain a complete catalog of sources of VHE γ -rays found by *Fermi*. The final photon list used in the analysis includes 2709 photons with $|b| \geq 10^\circ$.

Photons detected by *Fermi*/LAT are divided into two types – *front*- and *back*-converting. Photons that pair-convert in the top 12 layers of the tracker are classified as front-converting, in the other case they are back-converting (Abdo et al., 2010b). At the same energy front-converting photons have somewhat better PSF¹. We take this fact into account and consider the sets of

1028 front- and 1681 back- converted photons separately in our correlation analysis.

If the sky region around the source is not too crowded, the point spread functions of individual *Fermi* sources do not overlap at the energies above ~ 1 GeV. Besides, at high Galactic latitudes the strength and complexity of diffuse Galactic γ -ray background at the energies above 1 GeV is largely reduced (compared to the low-latitude / low-energy background). Taking into account these two facts we adopt a simplified procedure for the extraction of the source spectra. For each source and each energy we first calculate the number of source counts within a circle of the radius equal to the 95% containment circle of the LAT PSF and calculate the LAT exposure within this circle using *gtexposure* tool. To estimate the diffuse sky background at the position of the source we calculate the number of background counts in a ring with the outer radius 3° and the inner radius equal to the 95% containment radius of the LAT PSF, centered on the source. We verify if the region used for background estimate contains point γ -ray sources (see e.g. the special case of the source RBS 76 discussed in section 6). If a source from the 1-st year *Fermi* catalog, or a new source is present in the default background estimate region, we either exclude a circle of the radius equal to the 95% containment radius of the LAT PSF around this source from the background estimate region, or displace the background estimate region altogether, so that it does not intersect with the 95% containment radius of the LAT PSF around the “contaminating” source. We have verified that the results obtained using such an intuitively simple spectral extraction procedure (similar to the one commonly used in X-ray astronomy) are consistent with those obtained via spectral extraction using likelihood analysis in narrow energy bins and/or likelihood analysis in the wide energy range using a pre-defined broad-band spectral model.

3. Correlation between arrival directions of $E \geq 100$ GeV photons and sources from the 1-st year *Fermi* catalog

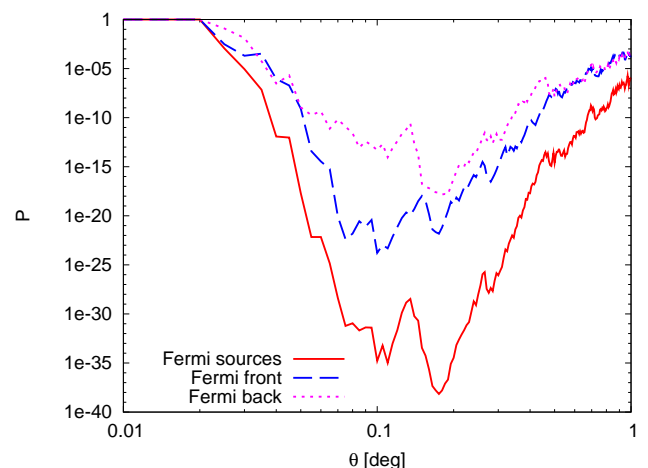


Fig. 1. Dependence on the chance probability of correlation between arrival directions of $E \geq 100$ GeV photons and positions of *Fermi* sources as a function of the radius of the search circle. Solid curve corresponds to all photons. Dashed and dotted curves correspond to respectively front and back converted photons.

¹ http://www-glast.slac.stanford.edu/software/IS/glast_lat_performance.htm

In order to find sources of $E \geq 100$ GeV γ -rays which individually cannot be recognized in the *Fermi* data in this energy band, we apply a method similar to the one discussed by Dingus & Bretsch (2001) and Gorbunov et al. (2005). Using this method, sources producing just a few photons could be identified. A fraction of identified sources could be false detections due to a chance coincidence between the source position and arrival direction of a background photon. The fraction of positive-to-false detections could be readily estimated. Real sources should largely outnumber the false source detections. This makes the list of sources contributing to the correlation a valuable "input catalog" for the observations with ground based γ -ray telescopes which are more sensitive than *Fermi* in the VHE γ -ray band, but, contrary to *Fermi*, do not have all-sky survey capabilities.

As a first choice, we took the 1-st year *Fermi* catalog as an input catalog for the correlation analysis (Abdo et al., 2010a). The catalog contains 1451 sources, 1024 of which are objects with $|b| \geq 10$ degrees. Removing 7 confirmed VHE γ -ray sources from the list of Neronov et al. (2010) (IC 310 is not in the *Fermi* catalog), we obtain an input catalog of $N_{\text{source}} = 1017$ sources.

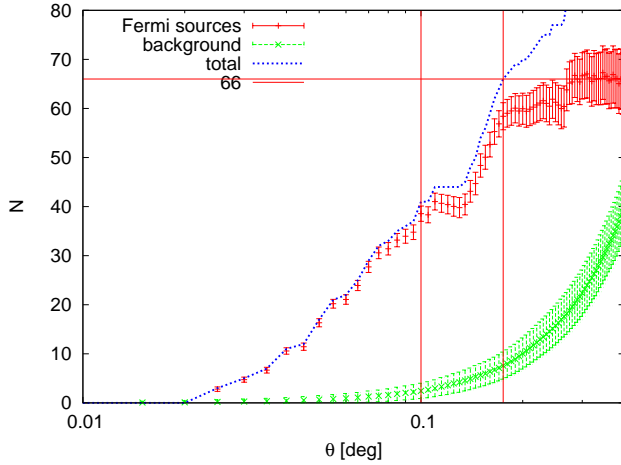


Fig. 2. Number of events which come from *Fermi* sources as a function of the radius of the search circle (red data points). Error bars indicate fluctuations of background in determination of signal from the sources. Average number of background photons is shown with green line. Vertical line at 0.1 degree is the radius of 68 % containment circle of *Fermi* PSF. Vertical line at 0.175 degree shows the position of the dip in the probability shown in Fig. 1. Horizontal line shows the asymptotic number of photons from all the sources.

The probability for a γ -ray to come within given distance θ from position of one source in the catalog is estimated as the ratio of the area of the circle of radius θ and the part of the sky at $|b| \geq 10^\circ$:

$$p_1 = \frac{\pi\theta^2}{4\pi(1 - \cos(80^\circ))} \simeq 9.2 \cdot 10^{-7} \left[\frac{\theta}{0.1^\circ} \right]^2 \quad (1)$$

The total probability for a photon to come within angle θ from position of one of the catalog sources is then

$$p = N_{\text{source}} \cdot p_1 = 9.3 \cdot 10^{-4} \left[\frac{N_{\text{source}}}{1017} \right] \left[\frac{\theta}{0.1^\circ} \right]^2 \quad (2)$$

Probability that K or more photons from $N_\gamma = 2709$ γ -rays come within the angle θ from any of sources in the catalog by chance is given by binomial probability

$$P(\theta) = \sum_{k=K}^{N_{\text{tot}}} p^k (1-p)^{N_\gamma-k} \frac{N_\gamma!}{(N_\gamma-k)!k!} \quad (3)$$

In Fig. 1 we plot this probability as a function of angle θ . The probability that γ -rays with energies higher than 100 GeV come from the directions close to the positions of *Fermi* sources by chance is $P < 10^{-38}$, i.e. the chance coincidence hypothesis is firmly ruled out.

The function $P(\theta)$ has two minima at around 0.1 degree and 0.175 degrees. This is explained by the fact that precision of determination of arrival direction for the front and back converted γ -rays is different. To verify this we split the whole photon list into two parts corresponding to the front and back converted γ -rays and plot the contributions of those photons separately. From Fig. 1 one can see that minimum at 0.1 degree is due to front photons, while minimum at 0.175 degrees is due to both front and back photons.

In Fig. 2 we plot the number of source photons with arrival directions within the angle θ from the catalog of *Fermi* sources and compare it to the expected number of background events within the same distance from the sources. To estimate the number of background events we used two alternative methods. First, we estimated the expected background near each source counting all photons within 10 degrees from it and estimating the fraction of photons which come within the angle θ . This method can be used only for $\theta \leq 0.5^\circ$. For $\theta \geq 0.5^\circ$ circles around *Fermi* sources cover significant fraction of the sky and overlap. In the second method we estimated the background by generating 2709 photons in the sky outside of Galactic plane $|b| > 10^\circ$, following *Fermi* exposure, estimated using *gtexposure* tool, and averaging over many Monte Carlo simulations. Both methods gave similar results for small angles.

Vertical lines in Fig. 2 show angular positions of the two minima of probability seen in Fig. 1. The minima correspond to the places where the steep rise of the number of signal events changes to a plateau. Asymptotic of the signal counts at large θ gives an estimate of the total number of γ -rays contributing to the correlation. One can see that only ~ 66 out of 2709 events come from the known *Fermi* sources. $N_{S, 0.1} \simeq 40$ of these 66 events are displaced by less than 0.1° from the catalog source position. In this circle one expects only $N_{B, 0.1} \simeq 2.5$ background events. No more than 6 background photons are expected at the 95% confidence level and no more than 8 background photons are expected at the 99.5% confidence level. The number of events contributing to the correlation within $\theta = 0.175^\circ$ circle is $N_{S, 0.175} \simeq 66$, while the expected number of background events is $N_{B, 0.175} \simeq 7.7$ (12 at 95% confidence level, 15 at 99% confidence level).

4. Catalog of extragalactic VHE γ -ray sources

The list of sources contributing to the correlation signal within $\theta = 0.1^\circ$ is given in Table 1. There are $N_{\text{Source}, 0.1} = 46 - 7 = 39$ such sources, if the sources from the list of Neronov et al. (2010) are excluded. On average, for $N_\gamma = 2709$, only $p \cdot N_\gamma \simeq 2.5$ photons could happen to be at the distance $\theta \leq 0.1^\circ$ from a catalog source by chance. This means that 2 – 3 out of 39 new VHE γ -ray sources listed in Table 1 are expected to be false detections (and no more than 6[8] sources are false detections at the 95% [99.5%] confidence level).

	IFGL	RA	Dec	N_{68} 30–100	P_{68} 30–100	N_{68} 100–300	N_{min} [N_{95}]	P 100–300	Type ¹	Name2	z
1	J0033.5-1921	8.3913	-19.3650	6	$9.8 \cdot 10^{-15}$	1b	1	$2.3 \cdot 10^{-5}$	BL V	RBS 76	0.61
2	J0054.9-2455	13.7337	-24.9290	0	–	1f		$2.8 \cdot 10^{-3}$			
3	J0110.0-4023	17.5250	-40.3887	1	$1.2 \cdot 10^{-2}$	1f		$1.8 \cdot 10^{-3}$			
4	J0209.3-5229	32.3392	-52.4907	2	$8.1 \cdot 10^{-5}$	1f		$2.9 \cdot 10^{-3}$	BL Vf	BZB J0209-5229	
5	J0213.2+2244	33.3225	22.7489	2	$1.2 \cdot 10^{-4}$	1b		$2.2 \cdot 10^{-3}$	QSO	CLASS J0212+2244	
6	J0222.6+4302	35.6681	43.0385	14	$3.1 \cdot 10^{-35}$	3f1b	1	$3.1 \cdot 10^{-12}$	BL V	3C 66A	0.444
7	J0237.5-3603	39.3788	-36.0530	3	$1.8 \cdot 10^{-7}$	1b		$2.1 \cdot 10^{-3}$	BL V	RBS 334	
8	J0303.5-2406	45.8890	-24.1124	8	$4.8 \cdot 10^{-21}$	1f	[1]	$1.7 \cdot 10^{-4}$	BL Vf	PKS 0301-243	0.26
9	J0315.9-2609	48.9933	-26.1581	1	$1.2 \cdot 10^{-2}$	2b		$2.5 \cdot 10^{-6}$	BL V	RX J0316.2-2607	0.443
10	J0316.3-6438	49.0996	-64.6411	0	–	1b		$1.2 \cdot 10^{-3}$			
11	J0325.9-1649	51.4780	-16.8174	0	–	1b		$2.1 \cdot 10^{-3}$	BL V	RBS 421	0.29
12	J0338.8+1313	54.7212	13.2314	0	–	1b		$2.9 \cdot 10^{-3}$			
13	J0416.8+0107	64.2069	1.1244	0	–	1f		$2.2 \cdot 10^{-3}$	BL Vf	2E 0414+0057	
14	J0428.6-3756	67.1567	-37.9412	3	$5.2 \cdot 10^{-7}$	1f		$2.4 \cdot 10^{-3}$	BL	PKS 0426-380	1.11
15	J0505.9+6121	76.4853	61.3527	1	$1.8 \cdot 10^{-2}$	1f	[2]	$8.3 \cdot 10^{-7}$			
16	J0507.9+6738	76.9931	67.6367	11	$6 \cdot 10^{-27}$	1f1b	1	$5.6 \cdot 10^{-6}$	BL V	1ES 0502+675	0.341
17	J0543.8-5531	85.9512	-55.5301	1	$1.6 \cdot 10^{-2}$	1b		$3.1 \cdot 10^{-3}$	BL V	BZB J0543-5532	
18	J0650.7+2503	102.6817	25.0622	1	$8.6 \cdot 10^{-3}$	1f	[1]	$1.1 \cdot 10^{-4}$	BL V	1ES 0647+250	0.203
19	J0710.6+5911	107.6595	59.1853	3	$1.5 \cdot 10^{-6}$	1f		$1.6 \cdot 10^{-3}$	BL	BZB J0710+5908	0.125
20	J0721.9+7120	110.4794	71.3448	6	$8.5 \cdot 10^{-14}$	1f		$3.1 \cdot 10^{-3}$	BL Vf	S5 0716+71	0.3
21	J0745.2+7438	116.3215	74.6415	0	–	1b		$3.4 \cdot 10^{-3}$	BL V	1ES 0737+746	0.315
22	J0809.4+3455	122.3539	34.9331	0	–	1f		$2.4 \cdot 10^{-3}$	BL Vf	B2 0806+35	0.0825
23	J0809.5+5219	122.3856	52.3178	3	$9.0 \cdot 10^{-7}$	1f1b		$4.4 \cdot 10^{-6}$	BL Vf	1ES 0806+524	0.138
24	J0816.4-1311	124.1121	-13.1933	3	$7.6 \cdot 10^{-8}$	1f		$1.4 \cdot 10^{-3}$	BL Vf	BZB J0816-1311	
25	J0905.5+1356	136.3916	13.9483	1	$1.3 \cdot 10^{-2}$	1b		$3.3 \cdot 10^{-3}$	AGN	CRATES J0905+1358	
26	J0915.7+2931	138.9412	29.5319	3	$5.3 \cdot 10^{-7}$	1f		$2.1 \cdot 10^{-3}$	BL Vf	B2 0912+29	
27	J0953.0-0838	148.2673	-8.6461	2	$6.7 \cdot 10^{-5}$	1f		$2.4 \cdot 10^{-3}$	BL Vf	RXS J09530-0840	
28	J0957.7+5523	149.4315	55.3922	4	$7.3 \cdot 10^{-9}$	1f		$3.1 \cdot 10^{-3}$	QSO	4C +55.17	0.8955
29	J1015.1+4927	153.7885	49.4526	5	$1.4 \cdot 10^{-11}$	1f	1	$3.4 \cdot 10^{-5}$	BL V	1ES 1011+496	0.212
30	J1104.4+3812	166.1247	38.2108	51	0	13f7b	3[1]	0	BL V	Mkn 421	0.03
31	J1117.1+2013	169.2993	20.2222	3	$3.7 \cdot 10^{-7}$	1f		$2.5 \cdot 10^{-3}$	BL Vf	CRATES J1117+2014	0.1
32	J1217.7+3007	184.4463	30.1206	2	$1.4 \cdot 10^{-4}$	1f		$2.5 \cdot 10^{-3}$	BL V	B2 1215+30	0.13
33	J1224.7+2121	186.1987	21.3633	0	–	1f		$1.7 \cdot 10^{-3}$	FSRQ	4C +21.35	0.432
34	J1337.7-1255	204.4336	-12.9289	0	–	1f		$1.3 \cdot 10^{-3}$	FSRQ	PKS 1335-127	0.539
35	J1437.0+5640	219.2617	56.6720	3	$8.3 \cdot 10^{-7}$	1f		$3.0 \cdot 10^{-3}$	BL	BZB J1436+5639	0.15
36	J1555.7+1111	238.9383	11.1921	25	0	2f2b	1	$2.7 \cdot 10^{-12}$	BL V	PG 1553+113	
37	J1653.9+3945	253.4897	39.7527	14	$7.2 \cdot 10^{-37}$	9f	1	$9.4 \cdot 10^{-29}$	BL V	Mkn 501	0.0336
38	J1722.5+1012	260.6494	10.2144	0	–	1f		$2.2 \cdot 10^{-3}$	FSRQ	CRATES J1722+1013	
39	J1744.2+1934	266.0710	19.5706	1	$1.9 \cdot 10^{-2}$	1b		$2.2 \cdot 10^{-3}$	BL V	1ES 1741+196	0.083
40	J1824.6+1013	276.1739	10.2180	0	–	1f		$1.7 \cdot 10^{-3}$			
41	J2000.0+6508	300.0215	65.1334	5	$5.4 \cdot 10^{-11}$	1f	[1]	$1.4 \cdot 10^{-4}$	BL Vf	1ES 1959+650	0.048
42	J2004.8+7004	301.2074	70.0710	0	–	1b		$3.8 \cdot 10^{-3}$			
43	J2009.5-4849	302.3761	-48.8295	7	$4.6 \cdot 10^{-16}$	4f	[1]	$2.4 \cdot 10^{-15}$	BL V	PKS 2005-489	0.071
44	J2158.8-3013	329.7117	-30.2176	22	0	5f3b	1[1]	$1.2 \cdot 10^{-24}$	BL V	PKS 2155-304	0.117
45	J2314.1+1444	348.5487	14.7463	1	$1.6 \cdot 10^{-2}$	1f		$2.4 \cdot 10^{-3}$	AGN	BZU J2313+1444	1.319
46	J2322.6+3435	350.6540	34.5839	1	$1.9 \cdot 10^{-2}$	1f		$3.0 \cdot 10^{-3}$	BL	CRATES J2322+3436	0.098

Table 1. List of *Fermi* sources for which a $E \geq 100$ GeV photon is found within the 68% containment circle of radius 0.1° . 1-st column: *Fermi* source ID; 2-nd column: Right Accention; 3-rd column: Declination; 4-th column: number of photons in the 68% containment circle in 30-100 GeV band; 5-th column: chance coincidence probability to find given number of photons in the 68% containment circle in 30-100 GeV band; 6-th column: number of photons in the 68% containment circle in 100-300 GeV band; "f" marks front photons, "b" marks back photons; 7-th column: number of photons in the $\theta \leq 0.175^\circ$ circle around the source or in the 95% containment circle of the radius 0.3° (square brackets); 8-th column: chance probability to find given number of background photons within 0.1° and 0.175° [0.3°] circles around the source position; 9-th column: alternative name of the source; 10-th column: source redshift. Bold marks the sources which have been previously detected in the VHE band by ground-based γ -ray telescopes.

¹ BL – BL Lac type object; QSO – quasi-stellar object, AGN – active galactic nucleus, FSRQ – flat spectrum radio quasar; FR I – Fanaroff-Riley type I radio galaxy; V – also found from the correlation analysis with the BL Lac catalog; Vf – front photon contributes to the correlation signal with the BL Lac catalog.

It is not possible to know in advance which of the 39 sources from Table 1 are false detections. In principle, the 8 sources which have more than one photon within the 95% containment circle of the LAT PSF are not expected to be false detections, because the probability that 2 background photons come close to

one and the same source is much smaller than the same probability for just one background photon. Additional information which might help to single out the false detections could be obtained from comparison of the estimate of the source fluxes expected from the extrapolation of the measured spectral char-

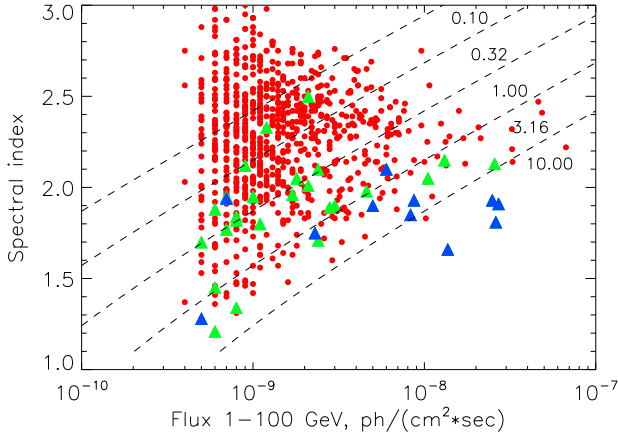


Fig. 3. Comparison of the distribution of fluxes and photon indices of *Fermi* sources of $E \geq 100$ GeV γ -rays (triangles) with those of all sources from the *Fermi* AGN catalog. Blue triangles mark known TeV γ -ray sources.

acteristics of the sources in the 1-100 GeV energy band with the simple estimates of the flux which produces 1 photon at $E \geq 100$ GeV within 1.5 year exposure with *Fermi*. In principle, a false detection might be spotted if the source contributing to the correlation has low flux and/or soft spectrum. This is illustrated by Fig. 3 in which the distribution of fluxes and photon indices of the AGN from the *Fermi* AGN catalog (Abdo et al., 2010c) is compared to the distribution of fluxes and photon indices of the sources from Table 1. Dashed lines show the combinations of the spectral parameters which are expected to give fixed number of photons in the 100-300 GeV band, assuming no high-energy cut-off in the spectrum.

One can see that the "candidates" for the false detections are the sources with softest spectra, which are 4C +21.35, PKS 1335-127 and CRATES J1722+1013. This is also clear from Fig. 4 in which the measurements of the source fluxes in 0.3-1 GeV, 1-3 GeV, 3-10 GeV and 10-100 GeV from the 1-st year *Fermi* catalog are compared with the estimates of the source fluxes in the 100-300 GeV band based on the number of $E \geq 100$ GeV detected photons from each source.

Although the significance of detection of individual sources of 1(2) photon in the 100-300 GeV band in Table 1 is around $3\sigma(4\sigma)$, some of the sources are detected with significance higher than 5σ in the adjacent 30-100 GeV energy band. The 5-th and 6-th columns of Table 1 show the numbers of photons and the chance coincidence probabilities derived from comparison of the expected number of background photons within $\theta \leq 0.12^\circ$ circles (corresponding to the 68% containment circle at 30 GeV) around the sources with the number of source photons in the 30-100 GeV band. For the sources which are detected with more than 5σ significance in the 30-100 GeV band we show more detailed spectra above 1 GeV, calculated using all publicly available data of *Fermi* collected from August 2008 to April 2010 (rather than 11 month data used for the analysis of the 1-st year *Fermi* catalog). One can see that for most of the sources the estimates of the source flux in the 100-300 GeV energy bin agree well with the extrapolation of the powerlaw spectrum from lower energies.

Maximum of the correlation signal (minimum of the chance probability) shown in Fig. 2 is achieved at the angle $\theta = 0.175^\circ$, corresponding to the 68% containment radius for the back type

events. Improvement of the correlation with the increase of θ from 0.1° to 0.175° means that there are more real events which came within the rings $0.1 \leq \theta \leq 0.175^\circ$ around their sources, than there are background events in these rings.

Table 2 lists the sources contributing to the correlation signal within $\theta \leq 0.175^\circ$ but not within $\theta \leq 0.1^\circ$. The number of background events in the ring $0.1^\circ \leq \theta \leq 0.175^\circ$ is estimated to be 5.4. This implies that 5 or 6 out of the 21 additional sources listed in Table 2 might be false detections.

It is important to note that only 16 out of 67 sources listed in Tables 1 and 2 are already known sources of VHE γ -rays detected by the ground-based γ -ray telescopes. Majority of the sources from Tables 1 and 2 are new real detections in the VHE band. Taking into account the fact that only 8 out of the 67 sources listed in Tables 1 and 2 are possible false detections, *Fermi* all sky survey at the energy $E_\gamma \geq 100$ GeV reveals 67-8-16=43 new extragalactic VHE γ -ray sources. This doubles the number of already known extragalactic VHE γ -ray sources ².

Another important point is that the $E \geq 100$ GeV γ -ray sources listed in Tables 1 and 2 are distributed over a broad range of redshifts. The "record" redshift of the VHE γ -ray source so far was $z \simeq 0.5$ for the possible detection of 3C 279 during a short several hour flare by MAGIC (Albert et al., 2008). In our Table 1 several sources have redshifts larger than 0.5.

5. Correlation between arrival directions of $E \geq 100$ GeV photons and sources from the 13th Veron catalog.

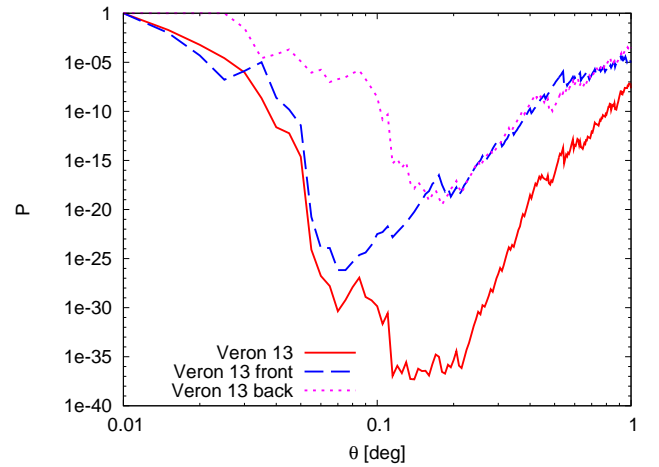


Fig. 5. Dependence on the chance probability of correlation between arrival directions of $E \geq 100$ GeV photons and positions of BL Lacs from Veron-Cetty & Veron (2010) catalog as a function of the radius of the search circle. Notations are the same as in Fig. 1.

Most of the $E > 100$ GeV sources listed in Tables 1 and 2 are BL Lac objects. These sources are known to be characterized by relatively hard spectra in the GeV energy band (Abdo et al., 2010c). It is, therefore, possible that some of the VHE γ -ray emitting BL Lacs escape detection in the GeV band, while being bright VHE γ -ray sources.

² See <http://tevcat.uchicago.edu/>

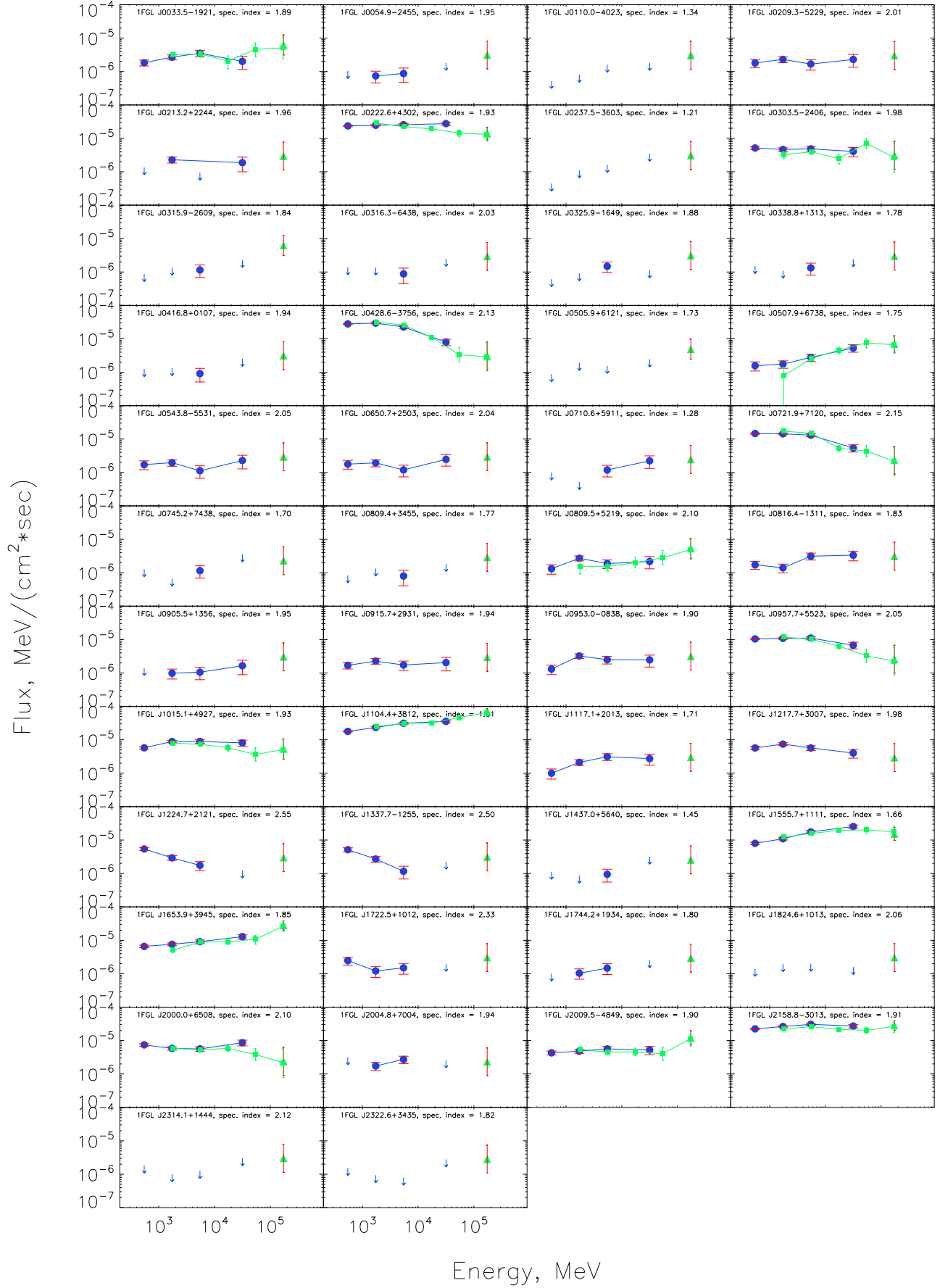


Fig. 4. Comparison of the spectra of the sources from Table 1 in the 0.3-100 GeV band with the estimated source fluxes in the 100-300 GeV band (green triangles). Blue circles (blue arrows) are the flux measurements (upper limits) from the 1-st year *Fermi* catalog. Green boxes are re-calculations of the source spectra using 1.5 yr exposure data set.

	1FGL	RA	Dec	N_{68} 30–100	P_{68} 30–100	N_{min} 100–300	P_{min} 100–300	Type	Name2	z
47	J0043.6+3424	10.9240	34.4060	1	$1.7 \cdot 10^{-2}$	1f	$7.8 \cdot 10^{-3}$			
48	J0203.5+7234	30.8940	72.5747	0	–	1f	$6.2 \cdot 10^{-3}$	BL	CGRaBS J0203+7232	
49	J0440.6+2748	70.1738	27.8151	0	–	1f	$4.8 \cdot 10^{-3}$		B2 0437+27B	
50	J0536.2-3348	84.0605	-33.8027	2	$1.1 \cdot 10^{-4}$	1f	$8.1 \cdot 10^{-3}$	BL Vf	FRBA J0536-3343	
51	J0803.1-0339	120.7800	-3.6544	1	$9.7 \cdot 10^{-3}$	1f	$3.1 \cdot 10^{-3}$			
52	J0856.6+2103	134.1578	21.0619	1	$1.1 \cdot 10^{-2}$	1b	$7.8 \cdot 10^{-3}$	FSRQ	OJ 290	2.106
53	J0909.2+2310	137.3005	23.1761	1	$1.5 \cdot 10^{-2}$	1b	$8.3 \cdot 10^{-3}$	BL V	RX J0909.0+2311	
54	J0942.1+4313	145.5303	43.2250	2	$1.4 \cdot 10^{-4}$	1b	$1.1 \cdot 10^{-2}$			
55	J1112.8+3444	168.2035	34.7363	0	–	1b	$1.1 \cdot 10^{-2}$	FSRQ	CRATES J1112+3446	1.9556
56	J1125.5-3559	171.3949	-35.9978	0	–	2b	$2.3 \cdot 10^{-5}$	AGN	CRATES J1125-3557	
57	J1136.9+2551	174.2362	25.8602	2	$1.1 \cdot 10^{-4}$	1f	$1.1 \cdot 10^{-2}$	BL V	BZB J1136+2550	0.2
58	J1253.0+5301	193.2646	53.0245	1	$1.7 \cdot 10^{-2}$	1b	$7.5 \cdot 10^{-3}$	BL V	CRATES J1253+5301	
59	J1325.6-4300	201.4143	-43.0110	1	$2 \cdot 10^{-2}$	1f	$6.1 \cdot 10^{-3}$	FR I	Cen A	0.00183
60	J1328.2-4729	202.0501	-47.4991	3	$1.1 \cdot 10^{-6}$	1f	$5.4 \cdot 10^{-3}$			
61	J1345.4+4453	206.3740	44.8965	0	–	1b	$6.9 \cdot 10^{-3}$	FSRQ	B3 1343+451	
62	J1426.9+2347	216.7495	23.7987	15	$1.1 \cdot 10^{-40}$	2b	$2.4 \cdot 10^{-5}$	BL V	PKS 1424+240	0.16
63	J1428.7+4239	217.1790	42.6568	6	$5.4 \cdot 10^{-15}$	1b	$7.0 \cdot 10^{-3}$	BL V	1ES 1426+428	0.129
64	J1553.9+4952	238.4886	49.8724	2	$1.1 \cdot 10^{-4}$	1b	$9.0 \cdot 10^{-3}$			
65	J1923.5-2104	290.8849	-21.0771	0	–	1f	$8.5 \cdot 10^{-3}$	FSRQ	OV -235	0.874
66	J2250.1+3825	342.5275	38.4328	3	$1.1 \cdot 10^{-6}$	1b	$6.3 \cdot 10^{-3}$	BL V	B3 2247+381	0.1187
67	J2325.8-4043	351.4613	-40.7184	1	$1.3 \cdot 10^{-2}$	1b	$7.2 \cdot 10^{-3}$	BL V	RXS J23247-4040	

Table 2. List of *Fermi* sources for which a $E \geq 100$ GeV photon is found within the radius $\theta = 0.175^\circ$, but not within $\theta = 0.1^\circ$. Notations are the same as in Table 1.

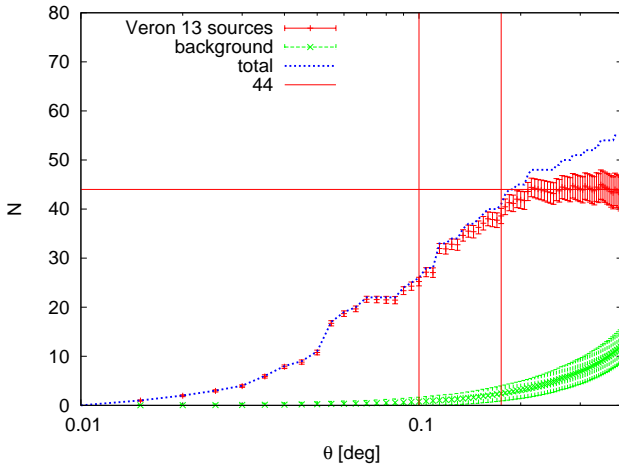


Fig. 6. Number of events which come from BL Lac sources as a function of the radius of the search circle. Notations are the same as in Fig. 2.

To search for the VHE γ -ray emitting BL Lacs with very hard spectra we have performed the correlation analysis similar to the one reported above for the 1-st year *Fermi* catalog also for the 13th Veron catalog of BL Lacs (Veron-Cetty & Veron, 2010). In order to select a complete sample of BL Lacs, we have adopted the prescription of Gorbunov et al. (2005) and made a cut on magnitude of objects $V < 18.0$, which leaves 316 BL Lacs. This set of objects includes 6 out of 7 known VHE γ -ray sources identified in the $E \geq 100$ GeV *Fermi* data by Neronov et al. (2010). Similarly to the analysis of the 1-st year *Fermi* catalog, we removed those objects and associated photons from analysis. We have also removed the 3 photons associated with IC 310. This leaves $N_{\text{source}} = 310$ BL Lac objects and 2709 photons.

The probability for a single photon to come by chance near one of the selected BL Lacs is $p = N_{\text{source}} \cdot p_1 = 2.7 \cdot 10^{-4}$.

$(\theta/0.1^\circ)^2$. The probability that K or more photons fall within an angle θ from one of the sources is calculated using Eq. 3. Fig. 5 shows this chance probability as function of θ . Similarly to the case of the analysis of 1-st year *Fermi* source catalog, the probability has a minimum at the angular resolution of LAT at the energies $E \geq 100$ GeV. 43 BL Lac out of 310 correlate with *Fermi* data within the angle $\theta \leq 0.175^\circ$ corresponding to the minimum of $P(\theta)$ from Fig. 1.

In Fig. 6 we compare the number of source photons to the number of background photons as functions of the angular distance to the BL Lacs. Asymptotical value of the signal events $N = 44$ is reached at the angular distance $\sim 0.2^\circ$. At the angle 0.1° 26 photons come from 25 sources, while only 0.77 of them are in average due to background. At 95 % C.L. there are 3 background photons and 4 at 99% confidence level. At the angular distance 0.175° 41 photons come from 35 sources, and 2.4 of them due to background in average. There are 6[7] background photons at the 95[99%] confidence level. 7 out of those 35 sources are not present in Tables 1 and 2. These seven sources are listed in the Table 3. Other sources which contribute to the correlation signal with both 1-st year *Fermi* and Veron-Cetty & Veron (2010) catalogs and marked as "V" in Tables 1 and 2.

We have also performed special analysis with only front photons and BL Lac catalog. In this case the correlation signal is maximal at $\theta \approx 0.07^\circ$ (see Fig. 5). At this angle there are 16 forward photons, which correlate with 16 BL Lac sources. Only 0.14 background photons are expected in this angle, which means that all the 16 sources are most probably real. At the 99% confidence level 2 of the 16 sources might be false detections. 12 of these 16 sources are marked as "Vf" in Tables 1 (11 sources) and 2 (1 source) and the remaining 4 are those which have front photons marked "f" in Table 3.

	Name	RA	Dec	$N_{0.175}$	z
1	V Zw 326	48.210	36.256	1b	0.071
2	B3 0651+428	103.682	42.799	1b	0.126
3	RXS J09130-2103	138.252	-21.054	1f1b	0.198
4	RXS J10162+4108	154.070	41.137	1b	0.281
5	SDSS J114023.48 +152809.7	175.098	15.469	1f	0.244
6	MS 12218+2452	186.101	24.607	1f	0.218
7	MS 13121-4221	198.764	-42.614	1f	0.105

Table 3. List of BL Lac sources from Veron-Cetty & Veron (2010) catalog for which a $E \geq 100$ GeV photon is found within the circle of radius 0.175° and which are not the 1-st year *Fermi* catalog sources.

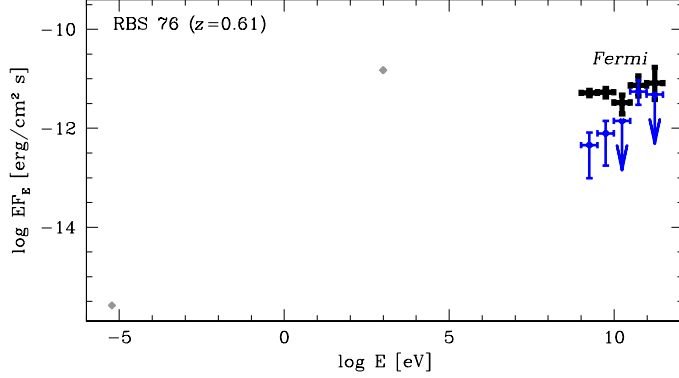


Fig. 7. Broad band spectrum of RBS 76. Grey data points are historical data from NED. Blue thin data points show the spectrum of an additional source FERMI J0535.7-1849 visible in Fig. 8.

6. Comments on individual sources

6.1. High redshift sources

Several sources in Table 1 have redshifts higher than the redshift of 3C 279, $z \approx 0.5$, which is the furthest known VHE γ -ray source (Albert et al., 2008). Study of the high redshift sources in the VHE band is interesting for the measurements of the density and cosmological evolution of the Extragalactic Background Light (EBL) (Gould & Schreder, 1967; Kneiske et al., 2004; Stecker et al., 2006; Mazin & Raue, 2007; Franceschini et al., 2008) and of the cosmological magnetic fields (Neronov & Semikoz, 2009; Neronov & Vovk, 2010). In this subsection we provide some details about the high redshift sources from Table 1.

RBS 76 at $z = 0.61$ has 2 photons within the distance 0.175° from the catalog source position. It is detected with significance more than 4σ in the 100-300 GeV band. The source is also detected with significance more than 7σ in the 30-100 GeV energy band.

Broad band spectrum of the source is shown in Fig. 7. The historical multiwavelength data are taken from the NASA Extragalactic database (NED)³. Comparing the radio, X-ray and γ -ray data one could conclude that the broad-band spectrum of the source fits into the general scheme of synchrotron-self-Compton or synchrotron-external Compton models with radio-to-X-ray emission being produced via synchrotron mechanism and γ -ray flux being generated via inverse Compton scattering.

In the course of investigation of the sky region around RBS 76 in the 1-300 GeV energy band we have discovered an additional source which is not reported in the 1-

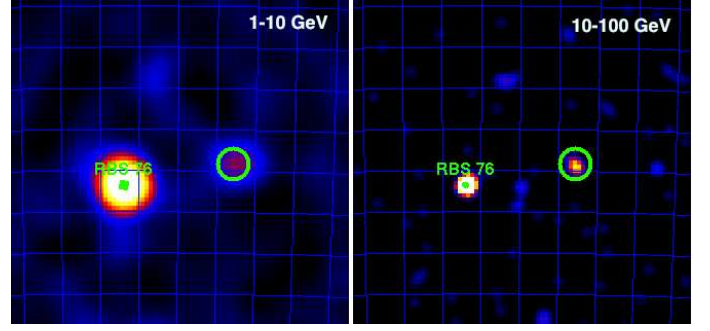


Fig. 8. Fermi count maps of the sky region around RBS 76 in 1-10 (left) and 10-100 GeV (right) energy bands. Circle shows the new unidentified *Fermi* source. Coordinate grid (RA, DEC) spacing is 1° .

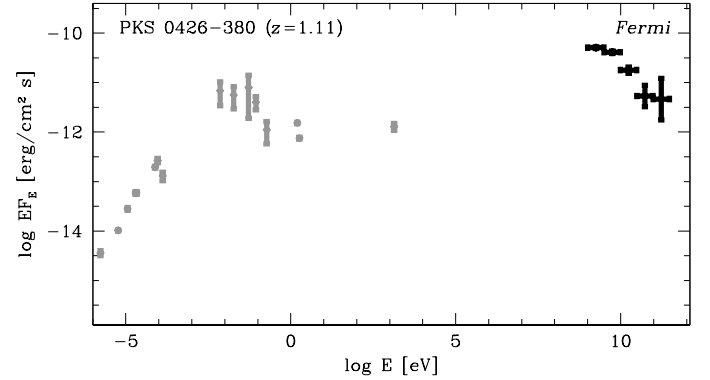


Fig. 9. Broad band spectrum of PKS 0426-380. Grey data points show historical data taken from NED.

st year *Fermi* catalog. The new source FERMI J0535.7-1849 has coordinates $RA=5.56 \pm 0.13$ $DEC=-18.86 \pm 0.12$. We have performed standard *Fermi* likelihood analysis (<http://fermi.gsfc.nasa.gov/ssc/data/analysis/>) and found that the Test Statistics (TS) value which characterizes the likelihood of source detection is $TS=136.5$, which corresponds to the source detection at approximately 11σ level (Mattox et al., 1996). There are no obvious low energy counterparts of the source. The source spectrum, shown in Fig. 7 is peaked in the 30-100 GeV band. The spectral characteristics of the source and the absence of low energy counterparts are consistent with the possibility that the source is a "blazar remnant" of the type discussed by Neronov et al. (2010b).

PKS 0426-380 at $z = 1.11$ is a bright source in the GeV energy band, with the flux reaching 10^{-10} erg/cm²s. Its γ -ray spectrum is relatively soft and is consistent either with a powerlaw with photon index $\Gamma \geq 2.5$ or with a cut-off powerlaw type spectrum. The γ -ray measurements are compared to the multiwavelength data on the source in Fig. 9. Similarly to the case of RBS 76, the overall spectrum of the source could be interpreted in terms of the synchrotron self-Compton or synchrotron external-Compton type models with radio-to-optical emission being produced via the synchrotron mechanism and X-ray-to- γ -ray emission being produced via inverse Compton scattering. Extremely high redshift of the source and possible presence of the high-energy cut-off in the spectrum might make detection of the source with ground-based γ -ray telescopes at the energies significantly larger than 100 GeV difficult.

³ <http://nedwww.ipac.caltech.edu/>

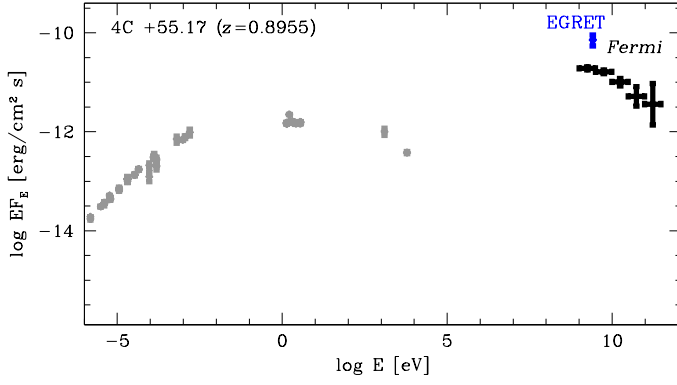


Fig. 10. Broad band spectrum of 4C +55.17. Grey data points show historical data from NED. Blue data point is the measurement of γ -ray flux by EGRET (Thompson et al., 1995).

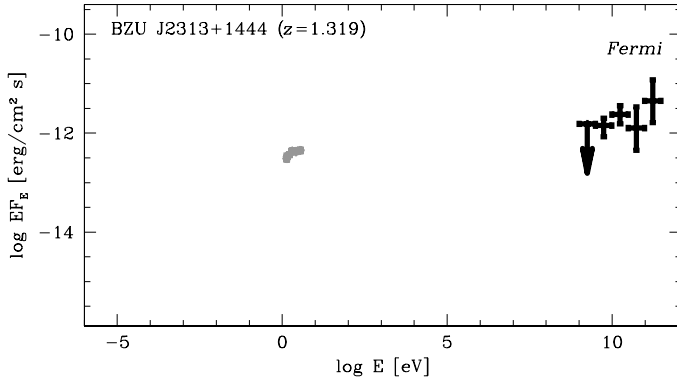


Fig. 11. Broad band spectrum of BZU J2313+1444. Grey data points show data from NED.

4C +55.17 at $z = 0.8955$ also has a relatively soft spectrum in the 1-300 GeV band. The γ -ray measurements are compared to the broad band data in Fig. 10. The source was previously detected in the 0.1-1 GeV band by EGRET. Comparison of the historical EGRET measurement with the *Fermi* measurement of the source flux shows that the source is variable at 10 yr time scale.

BZU J2313+1444 is formally the highest redshift source in Table 1, with $z = 1.319$. The source is relatively weak. Contrary to the other high-redshift sources, the significance of source detection in the 30-100 GeV band is less than 5σ . From Fig. 11 one can see that the source spectrum does not show a signature of high energy cut-off. This implies that the source might be an ideal candidate for the study of EBL evolution with redshift.

6.2. Sources detected at $\geq 4\sigma$ level at $E \geq 100$ GeV

Apart from the 8 high-confidence sources at $E \geq 100$ GeV found by Neronov et al. (2010) and the bright high-redshift sources discussed above, several other sources in tables 1 and 2 have detection significance higher than 4σ above 100 GeV. Below we list these sources and discuss some details of their broad band spectral energy distribution.

PKS 0301-243 at $z = 0.26$ has one back and one front-converted photon associated with the source above 100 GeV. The back photon is within the 95% containment circle of the radius $\theta = 0.3^\circ$. Taken together the two photons result in a $\approx 3.8\sigma$ detection of the source above 100 GeV. At the same time, the

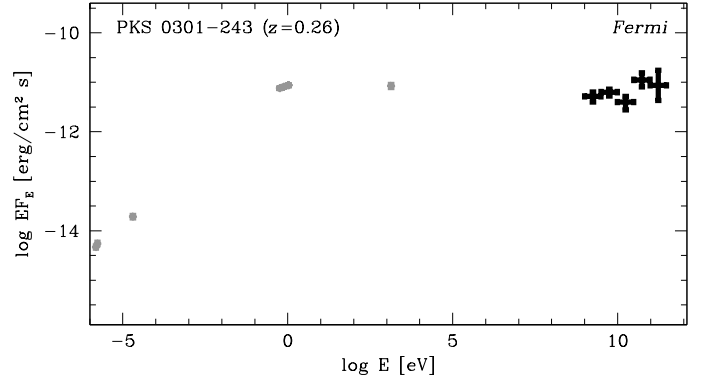


Fig. 12. Broad band spectrum of PKS 0301-243. Grey color shows historical data from NED.

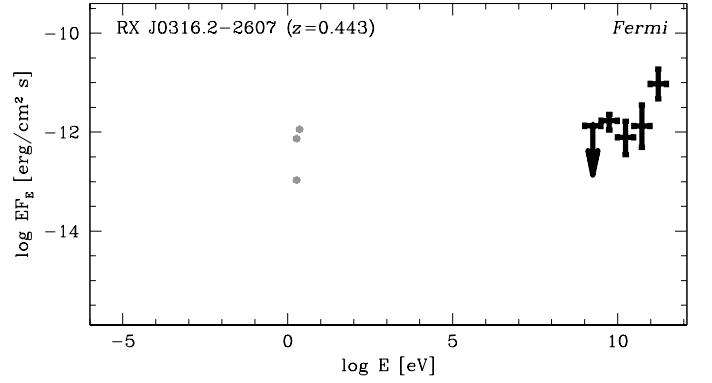


Fig. 13. Broad band spectrum of RX J0316.2-2607. Grey color shows historical data from NED.

source is also detected with high significance in the 30-100 GeV band. The broad band spectrum of PKS 0301-243, shown in Fig. 12, is consistent with the possibility that radio-to-X-ray emission are produced via synchrotron mechanism and 1-300 GeV emission via the inverse Compton mechanism.

RX J0316.2-2607 is a relatively high redshift ($z = 0.443$) source which has 2 back γ -rays within the distance $\theta = 0.1^\circ$. The chance coincidence probability of finding two photons within this distance from the source is 2.5×10^{-6} which implies detection significance 4.7σ above 100 GeV. From Fig. 13 one can see that the source has hard γ -ray spectrum without a signature of high-energy cut-off. The γ -ray energy flux from the source is comparable to the optical flux. Similarly to BZU J2313+1444, this source also might be an ideal candidate for the study of EBL and of cosmological magnetic fields.

1FGL J0505.9+6121 has 3 photons next to it within 0.22° . Formally, the chance probability of finding three photons inside this distance is $P = 8 \cdot 10^{-8}$, however, since detection angle was not defined a priori, it has to be penalized for this and the final probability is just 5σ (see Table 1), which still implies that the source is detected at $E \geq 100$ GeV individually, and not only within the population of *Fermi* sources from Table 1. It is also detected with significance higher than 5σ in the 30-100 GeV band. The spectrum of the source shown in Fig. 14 is consistent with a hard powerlaw (photon index harder than 2) up to the highest energy.

The object is located near the Galactic Plane at $b = +12^\circ$, so that it can be of Galactic origin. High level of Galactic diffuse

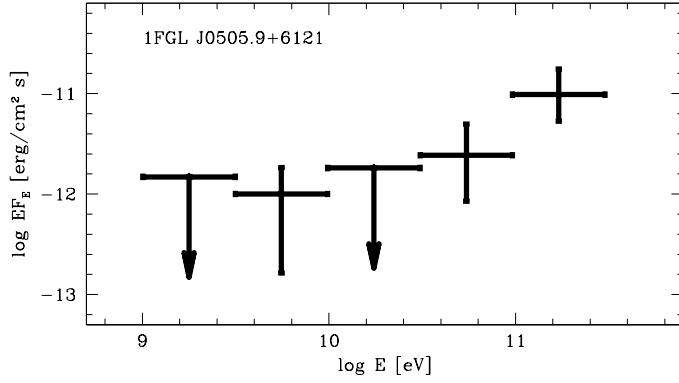


Fig. 14. *Fermi* spectrum of 1FGL J0505.9+6121.

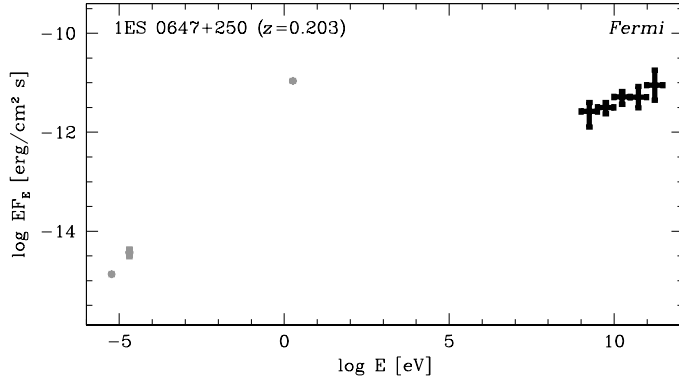


Fig. 15. Broad band spectrum of 1ES 0647+250. Grey color shows historical data from NED.

γ -ray background around the location of the source prevents its detection at lower energies $E \leq 1$ GeV.

Detailed multiwavelength observations are needed to constrain its nature. A possible candidate for the source identification is the radio- and X-ray loud AGN RX J0505.9+6113 (Brinkman et al., 1997) situated at the distance $7.6'$ from the catalog source position and at the distance 0.06° from the front $E \geq 100$ GeV photon.

1ES 0647+250 at $z = 0.201$ was already mentioned as a "candidate" TeV blazar in the analysis of Costamante & Ghisellini (2002), based on its broad band spectra properties. Fig. 15 demonstrates that the source has hard γ -ray spectrum, with no signature of cut-off up to 300 GeV. This assures that it should be readily detectable with the ground based γ -ray telescopes.

6.3. Sources from the BL Lac catalog

RX J09130-2103 has 2 γ -rays with energies $E \geq 100$ GeV within 0.1° distance. One of the γ -rays is a front type γ -ray, for which the 68% containment circle has smaller radius. The front γ -ray is at the distance 0.01° from the catalog source position and a back photon at 0.03° . The field of the radius 10° around the source contains 20 photons at the energies above 100 GeV. The overall chance probability of finding a front and back photons within the 68% containment circles of the front and back photons is $\approx 10^{-5}$.

In spite of the fact that the source is not reported in the 1-st year *Fermi* catalog, it is detected with *Fermi* also at the energies below 100 GeV. Standard likelihood analysis in the energy range 1-300 GeV gives the TS value 80 which corresponds to the significance of source detection $\approx 9\sigma$.

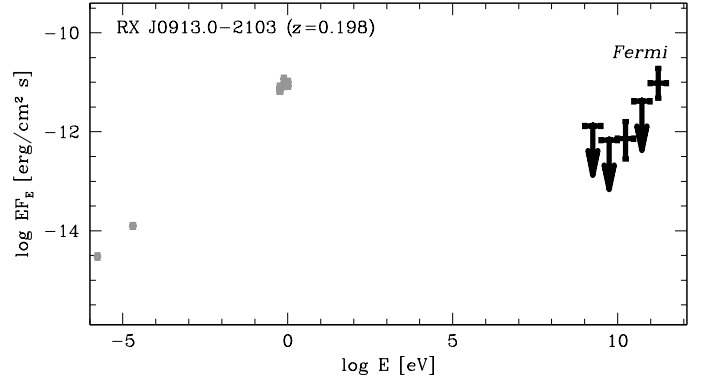


Fig. 16. Broad band spectrum of RX J0913.0-2103. Grey data points show historical data from NED.

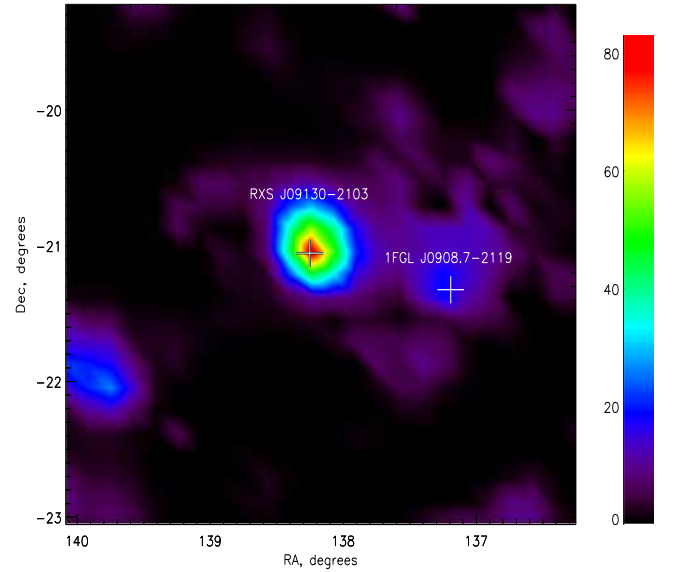


Fig. 17. TS map of the region $2^\circ \times 2^\circ$ in the energy band above 1 GeV around the position of RX J0913.0-2103.

The map of TS values in the region $2^\circ \times 2^\circ$ around the source is shown in Fig. 17. The TS values were calculated for the model of source distribution in the region 14° around RX J09130-2103 in which all the the 1-st year *Fermi* source catalog sources except for 1FGL J0908.7-2119 were included and one additional source was allowed to have variable position. One can see that the TS value at the position of RX J09130-2103 is much larger than that at the position of 1FGL J0908.7-2119 which is only marginally detected above 1 GeV.

The broad band spectrum of the source is shown in Fig. 16. One can see that the γ -ray spectrum of the source is hard, which explains its non-detection in the first 11 months of operation of *Fermi*.

MS 12218+2452 has a front photon at the distance 0.04 from the catalog source position. The source is also not reported in the 1-st year *Fermi* catalog, but is detected in the 1.5 yr exposure with TS value 80, which corresponds to the $\approx 9\sigma$ significance of the source detection.

The map of TS values in the region of the size $1^\circ \times 1^\circ$ at the energies $E \geq 1$ GeV around the source position is shown in Fig. 19. To construct this map we included all the sources from the

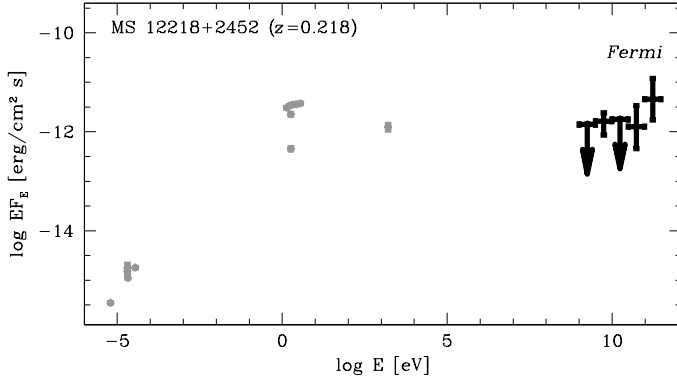


Fig. 18. Broad band spectrum of MS 12218+2452. Grey data points show historical data from NED.

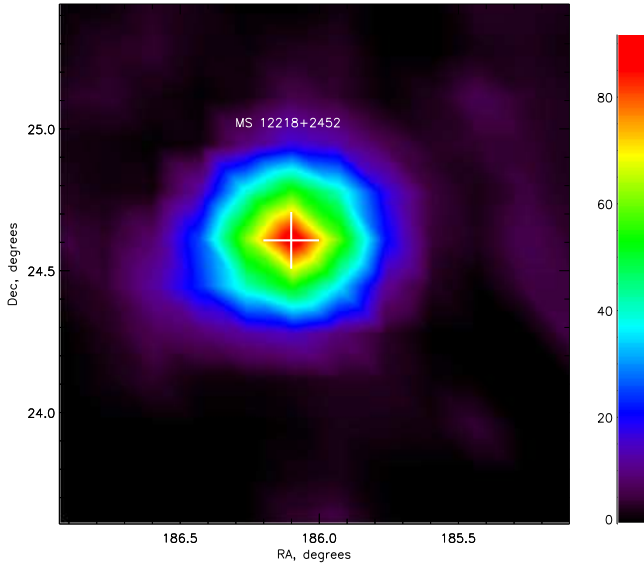


Fig. 19. TS map of the region $1^\circ \times 1^\circ$ in the energy band above 1 GeV around the position of MS 12218+2452.

1-st year *Fermi* catalog situated at the distance $\theta \leq 14^\circ$ from the source position into the model of source distribution on the sky. One can see that the source can be clearly in the TS map.

Fermi data are compared to the broad band archival data in Fig. 18. γ -ray flux from the source is comparable to the optical flux. The γ -ray spectrum does not show signatures of high-energy cut-off.

7. Discussion and conclusions

Study of cross correlation of the arrival directions of the highest energy photons ($E \geq 100$ GeV) detected by *Fermi* with the catalog of sources detected at lower energies $E < 100$ GeV proves to be an efficient way to find new γ -ray sources observable in the VHE γ -ray band. Such a study is complementary to the pointed observations of selected γ -ray sources with the ground-based γ -ray telescopes. It has enabled production in an all sky survey of high Galactic latitude VHE γ -ray sky.

The high Galactic latitude sky survey above 100 GeV has revealed a large number of new VHE γ -ray sources. Addition of the new sources to all the sources previously detected with the ground based γ -ray telescopes doubles the number of known ex-

tragalactic VHE γ -ray sources. Similarly to already known VHE γ -ray sources, most of the new sources reported in Tables 1-3 are BL Lac type objects, a special type of AGN with jets closely aligned with the line of sight.

Majority of the sources listed in Table 1 are real new VHE γ -ray sources, only 2 or 3 sources are expected to be false detections due to the chance coincidence of arrival directions of γ -rays with the source position. Based on the analysis of the spectral properties of the source in the 0.3-100 GeV band, the most probable false detections in Table 1 are source # 33, 34 and 38. On the other side, several sources in Table 1 have more than one photon associated with them. These sources are detected with highest significance above 100 GeV. Apart from the known VHE γ -ray sources, the unidentified *Fermi* source 1FGL J0505.9+6121 is detected with significance close to 5σ significance above 100 GeV and the sources # 1, 8, 9 and 18 are detected with $\sim 4\sigma$ significance. In addition, BL Lacs with an associated front photon which are found to correlate with the Veron-Cetty & Veron (2010) catalog (marked by "Vf" in Table 1) should also be considered as high-confidence detections.

Table 2 lists 21 lower significance sources, among which 5 or 6 are most probably false detections. Similarly to Table 1, source marked "Vf" (# 50) which contributes with a front photon to the correlation with the BL Lac catalog should be considered as a higher significance detection. For the sources listed in this table, it is reasonable to accumulate larger exposure to single out false detections.

Table 3 lists VHE γ -ray emitting BL Lacs which are not listed in the 1-st year *Fermi* catalog, but contribute to the correlation of the *Fermi* VHE γ -rays with the BL Lac catalog of Veron-Cetty & Veron (2010). The absence in the *Fermi* catalog might be explained by the very hard spectra of these sources. We have demonstrated that 2 of the 7 sources listed in Table 3, the sources # 3 and 6 are, in fact, detected with significance $\sim 9\sigma$ in 1-300 GeV band. The source RX J09130-2103, which has 2 photons associated with it is individually detected with significance more than 4σ above 100 GeV. The other 3 sources which have a front photon associated with them should also be considered as most probable true detections.

Some of the new VHE γ -ray sources listed in Table 1 is situated at large redshifts $z \sim 1$. Our analysis of the γ -ray spectra of the high redshift sources shows that at least several of them do not show any signatures of high-energy cut-off up to 300 GeV. Typical fluxes of the sources listed in Tables 1-3 are at the level $EF_E(E \geq 100 \text{ GeV}) \geq (\text{few}) \times 10^{-12} \text{ erg/cm}^2 \text{ s}$, i.e. at the level of 0.1 Crab units. Such sources should be readily detectable with the ground based Cherenkov telescopes at the energies several hundreds of GeV. Larger collection area of the ground-based telescopes should result in the much higher signal statistics, which should allow a study of the detailed spectral properties of these new bright VHE γ -ray sources. We anticipate that detailed high sensitivity study of the high-redshift VHE γ -ray sources with the ground based γ -ray telescopes will open a possibility to study cosmological evolution of the BL Lac properties, of the EBL and of the associated evolution of galaxies producing the EBL (Gould & Schreder, 1967; Kneiske et al., 2004; Stecker et al., 2006; Mazin & Raue, 2007; Franceschini et al., 2008) as well as of cosmological intergalactic magnetic fields (Neronov & Semikoz, 2009; Neronov & Vovk, 2010).

References

- Abdo A.A., et al., 2010, arXiv:1002.2280
- Abdo A.A. et al., 2010, arXiv:1003.0895

- Abdo A.A. et al., 2010, arXiv:1002.0150
- Aharonian F.A. et al., 2005, *Science*, 307, 1938
- Aharonian F.A. et al., 2006, *Ap.J.*, 636, 777
- Albert J. et al., 2008, *Science*, 320, 1752
- Amenomori, M., *Ap.J.*, 633, 1005
- Atkins R. et al., 2004, *Ap.J.*, 608, 680
- Brinkman W. et al., 1997, *A&A*, 323, 739
- Costamante L., Ghisellini G., 2002, *A&A*, 384, 56
- Dingus B. L., Bretsch D.L., 2001, *AIP Conf. Proc.*, 587, 251
- Franceschini A., Rodighiero G., Vaccari, M., 2008, *A&A*, 487, 837
- Gorbunov D.S., Tinyakov P.G., Tkachev I.I., Troitsky S.V., 2005, *MNRAS*, 362, L30
- Gould R.J., Schreder G.P., 1967, *Phys. Rev. Lett.* 16, 252
- Kneiske T.M., Bretz T., Mannheim K., Hartmann D.H., 2004, *A&A*, 413, 807
- Mariotti M., 2010, *ATEL* 2510
- Mazin D., Raue M., 2007, *A&A*, 471, 439
- Mattox J.R. et al. 1996, *Ap.J.*, 461, 396
- Neronov A., Semikoz D.V., 2009, *Phys. Rev. D*, 80, 123012
- Neronov A., Semikoz D.V., Vovk Ie., 2010, arXiv:1003.4615 (submitted to *A&A*)
- Neronov A.N., Semikoz D.V., Kachelriess M., Ostapchenko S., Elyiv A., 2010b, arXiv:1002.4981 (submitted to *Ap.J.Lett*)
- Neronov A., Vovk Ie., 2010, *Science*, 328, 73
- Stecker F.W., Malkan M.A. Scully S.T., 2006, *Ap.J.* 648, 774
- Thompson D.J. et al., 1995, *Ap.J.S.*, 101, 259
- Veron-Cetty, M. P.; Veron, P., 2010, *A&A*, in print